Graphene-on-dielectric micromembrane for optoelectromechanical hybrid devices

Schmid, Silvan; Bagci, Tolga; Zeuthen, Emil; Taylor, Jacob M.; Herring, Patrick K.; Cassidy, Maja C.; Marcus, Charles M.; Villanueva Torrijo, Luis Guillermo; Amato, Bartolo; Boisen, Anja

Total number of authors:
15

Published in:
arXiv.org, e-Print Archive, Condensed Matter

Publication date:
2013

Document Version
Publisher's PDF, also known as Version of record

Graphene-on-dielectric micromembrane for optoelectromechanical hybrid devices

Silvan Schmid,[1] Tolga Bagci,[2] Emil Zeuthen,[2] Jacob M. Taylor,[3] Patrick K. Herring,[4] Maja C. Cassidy,[4] Charles M. Marcus,[5] Luis Guillermo Villanueva,[6] Bartolo Amato,[6] Anja Boisen,[6] Yong Cheol Shin,[7] Jing Kong,[7] Anders S. Sørensen,[2] Koji Usami,[2] and Eugene S. Polzik[2]

[1]*Department of Micro- and Nanotechnology, Technical University of Denmark, DTU Nanotech, DK-2800 Kongens Lyngby, Denmark*

[2]*QUANTOP, Niels Bohr Institute, University of Copenhagen, DK-2100 Copenhagen, Denmark*

[3]*Joint Quantum Institute/NIST, College Park, Maryland, USA*

[4]*School of Engineering and Applied Science, Harvard University, Cambridge, Massachusetts 02138, USA*

[5]*Center for Quantum Devices, Niels Bohr Institute, University of Copenhagen, DK-2100, Denmark*

[6]*Department of Micro- and Nanotechnology, Technical University of Denmark, DTU Nanotech, Building 345 East, DK-2800 Kongens Lyngby, Denmark*

[7]*Department of Materials Science and Engineering, Massachusetts Institute of Technology, Cambridge, Massachusetts 02139, USA*

Abstract

Due to their exceptional mechanical and optical properties, dielectric silicon nitride (SiN) micromembranes have become the centerpiece of many optomechanical experiments. Efficient capacitive coupling of the membrane to an electrical system would facilitate exciting hybrid optoelectromechanical devices. However, capacitive coupling of such SiN membranes is rather weak. Here we add a single layer of graphene on SiN micromembranes (SiN-G) and compare the electromechanical coupling and mechanical properties to bare SiN membranes and to membranes coated with an aluminium layer (SiN-Al). The electrostatic force to external coplanar electrodes of SiN-G membranes is found to be equal to that of the SiN-Al membranes and corresponds to the theoretical value calculated for a perfectly conductive membrane coating. Our results show that a single layer of graphene substantially enhances the electromechanical capacitive coupling of a SiN membrane without significantly adding mass, decreasing the mechanical quality factor or affecting the optical properties.

Hybrid devices capable of coupling different systems are presently one of the hot topics in quantum technologies [1, 2]. Recent proposals [3, 4] outline optoelectromechanical systems, where a mechanical resonator is strongly coupled to an optical and an electrical resonator at the same time. The centerpiece of these proposals is a mechanical micromembrane inside an optical resonator which is capacitively coupled to an LC circuit [3]. For these applications it is essential to have a strong electromechanical coupling relative to the mechanical properties of the membrane.

A key feature of SiN micromembranes is their ultrahigh quality factor (Q) reaching $10^6 - 10^7$, low mass and excellent optical transparency with losses less than 10^{-5} in the near infrared [5–7]. In order to not downgrade these essential properties it was proposed to use dielectric polarization forces on bare SiN membranes for the electromechanical coupling [3]. Such forces on a dielectric are however, inherently weaker than the forces on conductors. In this work, we deposit a single layer of graphene onto SiN membranes (SiN-G) and compare their mechanical properties and electromechanical coupling to bare SiN membranes and to membranes covered with an aluminium layer (SiN-Al) [8]. We show that this single layer of graphene allows superior electromechanical coupling without deteriorating the exceptional properties of SiN membranes. Importantly, our setup uses graphene in a floating electrode configuration. Thereby graphene is not in contact with a metal and the interaction happens electrostatically. In this fashion we avoid the large contact resistance associated with connecting graphene and a metal electrode [9–11].

We used commercial high and low-stress 50 nm thick Si_3N_4 membranes (Norcada Inc.) for both the SiN and SiN-G resonators. Single layer graphene was grown on copper foil using standard CVD techniques [12]. The graphene on copper was cut to size, the copper wet-etched and the graphene transferred to the surface of the membrane in the aqueous environment. A thin layer of PMMA was used to support the graphene during the etching and transfer process. Once dry, the PMMA layer was removed from the graphene using acetone vapor. The final structure was robust enough for subsequent fabrication steps, for instance for making a round opening window in the graphene for future optical cavity applications or lithographically defining gates for control of the carrier density and type. In the experiments described below we used membranes without the opening in the graphene layer. The Al covered membranes were fabricated in-house by standard cleanroom processing. The high-stress stoichiometric SiN layer is 100 nm thick. The aluminium layer is 50 nm thick

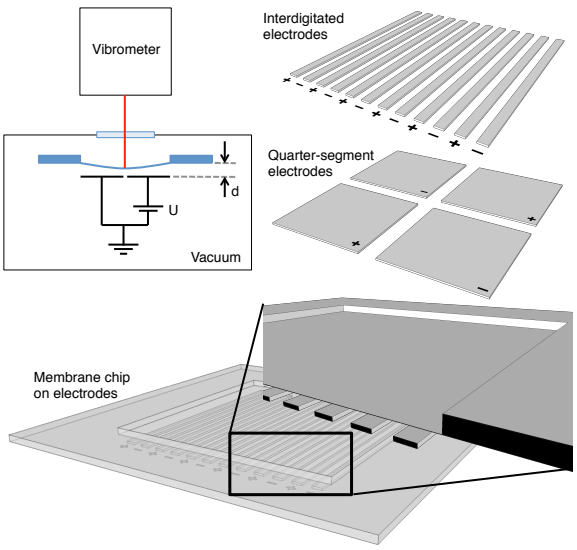

FIG. 1. Schematic drawing of the experimental setup. The micromechanical membranes are placed on top of coplanar electrodes. Two types of electrodes are used: interdigited finger electrodes and quarter-segment electrodes.

and it is patterned by a lift-off step. The Al layer could also be fabricated with a round hole in the center of the membrane for optical access. A small rim (5% of the membrane size) along the anchor of the membrane was spared out in order to minimize damping [8, 13].

Two types of coplanar electrode chips were used: interdigitated electrodes and quarter-segment electrodes. Schematic drawings of two types of electrodes are depicted in Fig. 1. The electrodes fabricated by standard cleanroom processing are made of a 200 nm thick gold layer sitting on borosilicate glass substrate or SiN covered silicon substrate. The membranes are placed membrane downwards onto the electrode. The electrode chips feature pillars with a height of 600 nm and 1 μ in order to define a small gap between membrane and electrodes. Optical measurements of the gap distance d and the membrane vibrations have been made with a white light interferometer (vibrometer MSA-500 from Polytec GmbH). The gap distance ranged from 3.5 to 14 μm which is larger than the height of the dedicated pillars. The larger measured distance can be ascribed to electrode chip unevenness coming from dirt and chip stress gradients and has been reduced down to the pillar height size in subsequent experiments.

The experimental setup is schematically depicted in Fig. 1. The membrane-electrode sandwich is placed in a vacuum chamber (pressure below 1×10^{-5} mbar) and is electrically

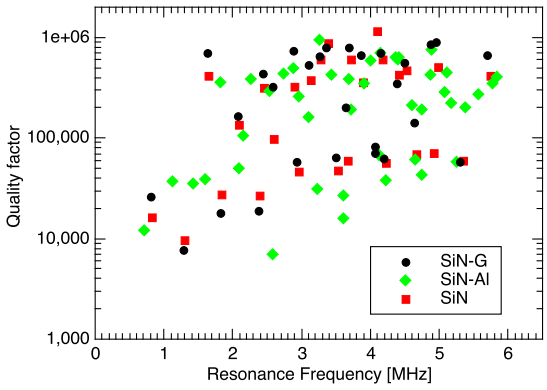

FIG. 2. Quality factors with increasing mode numbers of a SiN-G membrane compared to a bare SiN and a SiN-Al membrane. The membranes have a diameter of 0.5×0.5 mm^2 and are all made of high-stress stoichiometric SiN.

connected to an external voltage source. For quality factor measurements, the membranes were placed on a piezo for stimulation. The quality factors were extracted from the membrane ring-down time and the -3dB bandwidth of the resonance peak.

A key feature of micromechanical membranes is their Q of up to several million. Such high quality factors are a requirement for strong optomechanical coupling and for high resolution measurements. In the first experiment we compared the quality factors of the 3 different types of membranes. Fig. 2 shows the measured quality factors of a bare SiN, SiN-Al, and SiN-G membrane. On the SiN-Al membrane a rim of 5% of the membrane dimension remained uncoated, whereas graphene is fully covering the entire SiN-G membrane. The quality factors are highly mode dependent and the measured values are in correspondence with values measured by Yu et al. [8]. There are clearly two sets of Q-values. According to [8], the lower set (below $\sim$ 100000) is limited by clamping losses. The higher set is limited by intrinsic damping, such as bulk or surface losses. It can be seen from the measurements that there is no significant difference between the different membrane types in both sets. The graphene sheet seems to be mechanically invisible and it does not significantly contribute to the energy loss. Thus with graphene it is not required to spare out the membrane area close to the clamping edge as it is for metal layers. The additional metal layer of the SiN-Al membrane downshifts the resonance frequencies compared to the other two membranes, which makes a direct comparison difficult.

It is crucial for an efficient hybrid optoelectromechanical device to have strong electrome-

chanical coupling between the membrane and the electrical circuit. The electrostatic interaction for SiN membranes is due to dielectric polarization forces (the electric field interacts with a dielectric) [3, 14] and in some of the experiments presented here it is also due to the quasi-permanent electric charges in a dielectric. The interaction for SiN-Al [1] and SiN-G is due to the electrostatic force between conductors (the electric field interacts with charges on a conductor). Neglecting the effect of free charges on the membrane, the electrostatic force between a dielectric or conductive thin membrane and electrodes can generally be described by

$$F = cAf(d)U^2 \tag{1}$$

with A - the membrane area, U - the potential difference over the electrodes, c - the electrostatic force constant that characterizes the coupling performance, and $f(d)$ - a function describing the distance dependence of the force.

We extract the intrinsic coupling strength c of each membrane type from measuring the mechanical frequency shift due to the so-called spring softening effect which results in a quadratic frequency drop with the DC-bias voltage U_{DC}. The relative frequency shift is given by (see supplementary information)

$$\frac{\Delta\omega}{\omega_0} = -\alpha U_{DC}^2. \tag{2}$$

Using α found from the frequency shift data (2), the electrostatic force constant c can be calculated from

$$c = 2\alpha[-f'(d)]^{-1}h\rho\omega_0^2\eta^{-1} \tag{3}$$

with the membrane thickness h and the membrane mass density ρ; while η (of order unity) quantifies the spatial overlap between the membrane mode shape and the fixed electrodes, in particular compensating for the gap between quarter-segment electrodes and for the circular hole in the SiN-Al membranes' center (see supplementary information).

Here the coupling performance of SiN-G membranes is compared to that of the SiN and SiN-Al membranes using the two types of capacitor+membrane chips described above. In the first set, SiN and SiN-G membranes are coupled to interdigitated electrodes; in the second set, SiN-Al and SiN-G membranes are coupled to quarter-segment electrodes.

For the interdigitated electrode geometry and the range of membrane-capacitor distances d used in the experiments, the electrostatic force for both dielectric and perfectly conducting

membranes (an appropriate model for our SiN-G membranes) is well approximated by

$$f(d) = A_0^{-1} e^{-\kappa d} \tag{4}$$

with A_0 - a scaling constant with units of area. For the data presented below, we use $A_0 = 1\ \mu\mathrm{m}^2$ For our specific setup, we determined numerically that $\kappa = 1.05 \mu m^{-1}$ for both dielectric and perfectly conducting membranes.

In Fig. 3a the electrostatic spring softening of a SiN-G membrane on top of an interdigitated electrode is shown. From the fit parameter α obtained from this data the force constant c is calculated for the membranes using Eq. (3) and the exponential force law (4). The resulting average force constants for the bare SiN and SiN-G membranes on interdigitated electrodes are shown in the left part of Fig. 3c. SiN-G is seen to outperform SiN by a factor of 5.5. Also shown are the theoretical values determined semi-analytically for dielectric (SiN, $\varepsilon_\mathrm{r} = 7.6$) and perfectly conducting membranes; the average force constant of SiN-G is seen to be compatible with the latter.

Next, we use the quarter-segment coplanar electrodes with a SiN-Al or a SiN-G membrane as a floating electrode. The results of this set of experiments are well described by another force law (in the regime where d is smaller than the inter-electrode gap):

$$f(d) = 1/d^2. \tag{5}$$

The measured spring softening of a SiN-G membrane placed over quarter segment electrodes is shown in Fig. 3b. From the fit parameter α obtained from this data the force constant c is calculated for the conducting membranes again with Eq. (3) but now using the quadratic force law (5). On the right side of Fig. 3c the extracted average force constants of SiN-G and SiN-Al membranes are shown. The experimental values again agree well with the theoretical value for a perfect conductor. The large standard deviation of the force constant can be assigned to uncertainties in the distance d measurement and lateral misalignment which can contribute up to 20% error.

An additional complication with SiN membranes which is eliminated by using SiN-Al or SiN-G membranes is the accumulation of free charges on the dielectric SiN membrane. The charging has been investigated by increasing the DC voltage and then inverting the polarity. If quasi-static charges are present, a spring hardening (increase in oscillation frequency) instead of softening will be observed. The results of this experiment are shown in Fig. 4

with a bare SiN, a SiN-Al and a SiN-G membrane on interdigitated electrodes. From the observed spring hardening, shown in Fig. 4a, it can be concluded that free electric charges are indeed available on the bare SiN membranes. We note that the force on a charge is a function of the inverse of the distance ($\propto 1/d$) and may therefore be partly responsible for the somewhat higher value of the coupling constant c for SiN shown in Fig. 3c.

Fig. 4b and Fig. 4c present the results of the same charging experiment conducted with a SiN-G and with SiN-Al membranes, respectively. The absence of spring hardening for SiN-G shows that the single layer of graphene as well as the Al layer eliminates charging.

We performed further characterization of the SiN-G membranes by studying the dependence of the ac amplitude and the dc displacement on the coupling voltage (Fig. 5). If the AC driving voltage is small compared to the DC bias voltage, the electrostatic force becomes

$$F = c\frac{A}{d^2}(U_{DC} + U_{AC})^2 \approx c\frac{A}{d^2}(U_{DC}^2 + 2U_{AC}U_{DC}). \tag{6}$$

Thus the mechanical resonance peak amplitude is approximately a linear function of the DC voltage, for a fixed AC driving voltage, and the static deflection of the membrane is a quadratic function of the DC voltage. As seen from Fig. 5 the experimentally observed behavior supports the model.

In conclusion we have shown that SiN-G membranes with a single layer of graphene are promising canditates for efficient optoelectromechanical hybrid coupling devices. Furthermore, by using the graphene sheet on SiN in a floating electrode configuration, we overcome the unsolved problem of high contact resistance between metal electrodes and graphene. They show electromechanical coupling which is as good as for an ideal conductor. The enhanced electromechanical coupling of conductive membranes lowers the threshold for strong coupling, as predicted for dielectric membranes [3], accordingly. The single graphene layer is mechanically invisible and does not negatively influence the membrane performance. Unlike the real metal coating, graphene does not require patterning in order to maintain the highest mechanical quality factors of a bare SiN membrane. Also, unlike the metal coating, graphene does not add any noticeable mass to the membrane which is an advantage for high sensitivity applications. Finally, the use of graphene overcomes the complications of charging effects in SiN membranes, which has shown to be difficult to control.

ACKNOWLEDGEMENTS

We acknowledge funding from the DARPA program QUASAR, the EU project QESSENCE and the ERC projects INTERFACE and QIOS (under Grant Agreement n. 306576). The research leading to these results has received funding from the European Communitys Seventh Framework Programme (FP7/2007-2013) under grant agreement n211464-2 and it was further supported by the Villum Kann Rasmussen Centre of Excellence NAMEC under Contract No. 65286.

[1] J. D. Teufel, D. Li, M. S. Allman, K. Cicak, A. J. Sirois, J. D. Whittaker, and R. W. Simmonds. Circuit cavity electromechanics in the strong-coupling regime. *Nature*, 471(7337):204–208, March 2011.

[2] E. Gavartin, P. Verlot, and T. J. Kippenberg. A hybrid on-chip optomechanical transducer for ultrasensitive force measurements. *Nature Nanotechnology*, 7:509–514, June 2012.

[3] J. Taylor, A. Sørensen, C. Marcus, and E. Polzik. Laser Cooling and Optical Detection of Excitations in a LC Electrical Circuit. *Physical Review Letters*, 107(27):1–5, December 2011.

[4] C. A. Regal and K. W. Lehnert. From cavity electromechanics to cavity optomechanics. *Journal of Physics: Conference Series*, 264:012025, January 2011.

[5] J. D. Thompson, B. M. Zwickl, A. M. Jayich, F. Marquardt, S. M. Girvin, and J. G. E. Harris. Strong dispersive coupling of a high-finesse cavity to a micromechanical membrane. *Nature*, 452(7183):72–75, 2008.

[6] D. J. Wilson, C. A. Regal, S. B. Papp, and H. J. Kimble. Cavity Optomechanics with Stoichiometric SiN Films. *Phys. Rev. Lett.*, 103(20):207204, November 2009.

[7] T. J. Kippenberg and K. J. Vahala. Cavity Opto-Mechanics. *Optics Express*, 15(25):17172–17205, July 2007.

[8] P.-L. Yu, T. Purdy, and C. Regal. Control of Material Damping in High-Q Membrane Microresonators. *Physical Review Letters*, 108(8):1–5, February 2012.

[9] S. Russo, M.F. Craciun, M. Yamamoto, A.F. Morpurgo, and S. Tarucha. Contact resistance in graphene-based devices. *Physica E: Low-dimensional Systems and Nanostructures*, 42(4):677–679, February 2010.

[10] A. Venugopal, L. Colombo, and E. M. Vogel. Contact resistance in few and multilayer graphene devices. *Applied Physics Letters*, 96(1):013512, 2010.

[11] K. S. Novoselov, V. I. Falko, L. Colombo, P. R. Gellert, M. G. Schwab, and K. Kim. A roadmap for graphene. *Nature*, 490(7419):192–200, October 2012.

[12] Xuesong Li, Weiwei Cai, Jinho An, Seyoung Kim, Junghyo Nah, Dongxing Yang, Richard Piner, Aruna Velamakanni, Inhwa Jung, Emanuel Tutuc, Sanjay K Banerjee, Luigi Colombo, and Rodney S Ruoff. Large-area synthesis of high-quality and uniform graphene films on copper foils. *Science (New York, N.Y.)*, 324(5932):1312–4, June 2009.

[13] S. Schmid, K. D. Jensen, K. H. Nielsen, and A. Boisen. Damping mechanisms in high-Q micro and nanomechanical string resonators. *Physical Review B*, 84(16):1–6, October 2011.

[14] Silvan Schmid, Christofer Hierold, and Anja Boisen. Modeling the Kelvin polarization force actuation of micro-and nanomechanical systems. *Journal of Applied Physics*, 107(5):054510, 2010.

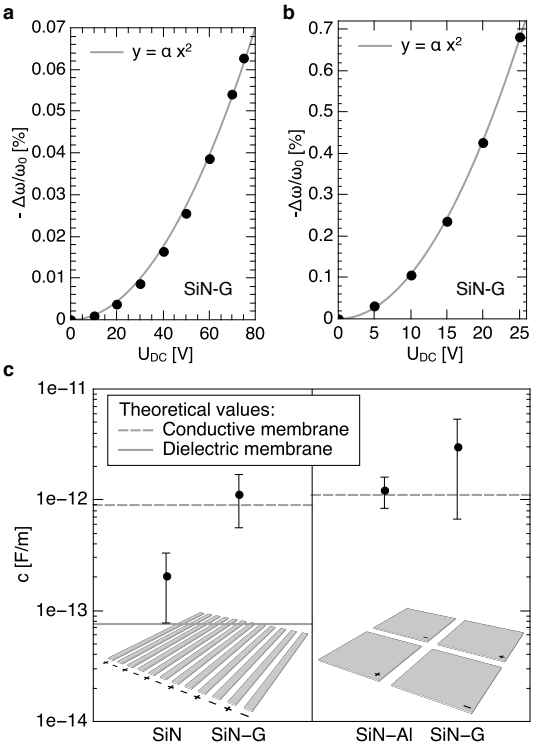

FIG. 3. Extraction and comparison of the electrostatic force constant c. a) Resonance frequency of fundamental mode of a 0.5×0.5 mm^2 SiN-G membrane on interdigitated electrodes as a function of DC voltage. The distance between membrane and electrodes is $d = 7.0$ μm. b) Resonance frequency fundamental mode of a 0.5×0.5 mm^2 SiN-G membrane on quarter-segment electrodes as a function of DC voltage. The distance between the membrane and electrodes is $d = 6.3$ μm. c) Comparison of force constants c (according to (3) using (4) and (5)) for different combinations of electrodes and membranes. On the left, c extracted for bare SiN (4 experiments) and SiN-G (3 experiments) membranes on interdigitated electrodes are shown. The electrode fingers are 4 μm wide with a gap of 2 μm between the fingers. To the right, c of SiN-Al (3 experiments) and SiN-G (4 experiments) on quarter-segment electrodes are shown, with a gap between the segments of 60 μm. The error bars represent the standard deviation of the conducted experiments. The solid and dashed grey lines represents the theoretical values for the scenario of a pure dielectric polarization force and an electrostatic force on the conductive membrane, respectively.

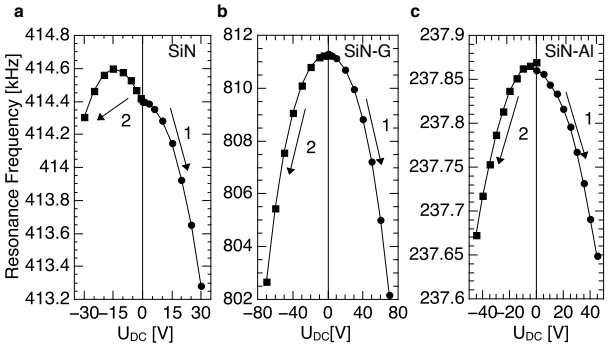

FIG. 4. Response of the resonance frequency of fundamental mode of a bare SiN, a SiN-G, and a SiN-Al membrane to DC polarity inversion. First the voltage was increased in the positive direction. Then the polarity was reversed and the voltage was increased in the negative direction. a) Response of a bare SiN membrane (1×1 mm^2, $d = 4.0\mu$m) on interdigitated electrodes; electrode fingers are 4 μm wide with a gap of 2 μm between the fingers. b) Response of a SiN-G membrane (0.5×0.5 mm^2, $d = 5.5\mu$m) on interdigitated electrodes; the electrode fingers are 4 μm wide with a gap of 5 μm between the fingers. c) Response of a SiN-Al membrane (1×1 mm^2, $d = 11$ μm) on quarter-segment electrodes. The resonance frequency was determined from the thermomechanical resonance peak.

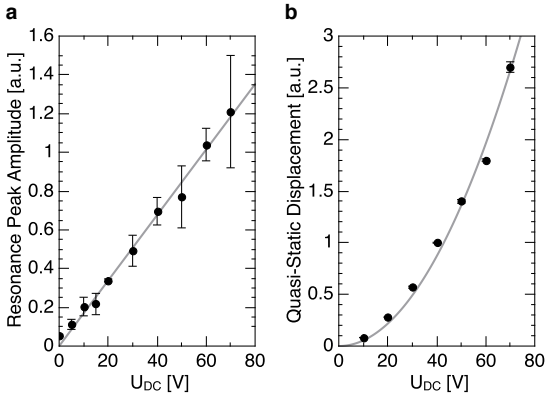

FIG. 5. Response of fundamental mode of a 0.5×0.5 mm^2 SiN-G membrane on interdigitated electrodes. Response of a) resonance peak amplitude and b) quasi-static displacement to DC bias voltage. The distance between membrane and electrodes is $d = 6.5$ μm. The electrode fingers are 4 μm wide with a gap of 5 μm between the fingers. The resonance peak amplitude was measured for a white noise signal of $U_{AC} = 10$ mV. The quasi-static displacement was measured with a rectangular signal at 10 kHz (which is far below the fundamental resonance frequency and can therefore be considered to be quasi-static). The error bars represent the standard deviation of 3 consecutive measurements. The grey lines represent a linear fit in a) and a quadratic fit in b).